

Comparing the coefficients of  $\partial_j\phi_\beta$  and  $\partial_j\partial_k\phi_\beta$  on the right-hand sides of Eqs. (15) and (A3), we obtain

$$\partial_0 R_{\alpha\beta}{}^j = -B_{\alpha\beta}{}^{0j} + B_{\beta\alpha}{}^{0j} + 2\partial_k C_{\alpha\beta}{}^{0kj}, \quad (\text{A4})$$

and

$$R_{\alpha\beta}{}^0\delta_{jk} = 2C_{\alpha\beta}{}^{0jk}. \quad (\text{A5})$$

Substituting from (A5), Eq. (A4) gives

$$\partial_0 R_{\alpha\beta}{}^j - \partial_j R_{\alpha\beta}{}^0 = -B_{\alpha\beta}{}^{0j} + B_{\beta\alpha}{}^{0j}. \quad (\text{A6})$$

Now the left-hand side is symmetric while the right-hand side is antisymmetric in  $\alpha$  and  $\beta$ . Both must, therefore, vanish. This proves Eq. (29).

### APPENDIX B

We start with Eq. (12) of Ref. 4; that is,

$$\langle 0 | [\phi_\alpha, U] | \beta \rangle = U_{\alpha\beta} \langle 0 | \phi_\beta | \beta \rangle. \quad (\text{B1})$$

This equation suggests the operator relation

$$[\phi_\alpha, U] = D_{\alpha\beta} \phi_\beta, \quad (\text{B2})$$

where  $D_{\alpha\beta}$  is some differential operator of the form

$$D_{\alpha\beta} = A_{\alpha\beta} + B_{\alpha\beta}{}^\mu \partial_\mu + C_{\alpha\beta}{}^{\mu\nu} \partial_\mu \partial_\nu + \dots \quad (\text{B3})$$

Now, Eq. (B2) gives

$$\begin{aligned} \langle 0 | [\phi_\alpha, U] | \beta \rangle &= \sum_\gamma \langle 0 | D_{\alpha\gamma} \phi_\gamma | \beta \rangle \\ &= \sum_\gamma g_{\alpha\gamma}(\phi_\beta) \langle 0 | \phi_\gamma | \beta \rangle \\ &= g_{\alpha\beta}(\phi_\beta) \langle 0 | \phi_\beta | \beta \rangle, \end{aligned} \quad (\text{B4})$$

where  $g_{\alpha\beta}(\phi)$  is some function of the momentum  $\phi$ . Comparing Eqs. (B1) and (B4), we get

$$g_{\alpha\beta}(\phi_\beta) = U_{\alpha\beta}. \quad (\text{B5})$$

Now if  $U_{\alpha\beta}$  is independent of momenta, then  $g_{\alpha\beta}$  should be a constant. This means that all terms on the right of Eq. (B3) except the first must vanish. We have therefore

$$[\phi_\alpha, U] = A_{\alpha\beta} \phi_\beta. \quad (\text{B6})$$

Now it is a straightforward calculation to obtain Eq. (44) without the second term on the right.

## Time-Like Momenta in Quantum Electrodynamics\*

STANLEY J. BRODSKY AND SAMUEL C. C. TING

*Department of Physics, Columbia University, New York, New York*

(Received 6 January 1966)

We have considered electron pair production by high-energy muons in a Coulomb potential as a test of quantum electrodynamics in the time-like region. If triple coincidence configurations are selected whereby the total momentum of the three final leptons is in the incident muon direction and the electron-positron pair is detected symmetrically with respect to the muon scattering plane, then the differential cross section is obtained in a simple analytical form. With these constraints it is seen that for a given effective mass of the pair, the contributions to the cross section involving timelike photon propagators become dominant as the muon scattering angle increases, although the cross section decreases slowly. If the constraints are relaxed, the cross section increases by orders of magnitude but the above features of the cross section persist. Thus, for a 10-BeV/c incident muon, nuclear charge  $Z=10$ , and effective pair mass 100 MeV, the cross section is nominally  $10^{-32}$  cm<sup>2</sup>/(MeV)<sup>2</sup>(sr)<sup>2</sup>, the time-like contribution gives more than 80% of the cross section, and the momentum transfer to the nucleus is less than 50 MeV/c over ranges of polar angles  $\Delta\theta=20$  mrad, azimuthal angles  $\Delta\phi=40^\circ$  and momenta  $\Delta P=1$  BeV/c. The characteristic behavior of the cross section is presented in graphical form and a simple method of computing the differential cross section (without involving large cancellations of gauge-variant quantities) is discussed.

**I**N this note we discuss the possibility of testing quantum electrodynamics when time-like photon momenta are involved in muon or electron pair production by incident high-energy  $\mu$  or  $e$  beams from presently available<sup>1</sup> proton or electron accelerators.

The lowest order Feynman diagrams for these trident<sup>2</sup>

\* This research was supported in part by the U. S. Atomic Energy Commission.

<sup>1</sup> The idea of obtaining a high-energy, high-intensity muon beam from the AGS accelerator to study quantum electrodynamics is due to L. M. Lederman, R. Cool, and J. Tinlot, Brookhaven National Laboratory Report No. PD-2 (1960) (unpublished).

<sup>2</sup> J. D. Bjorken and S. D. Drell, Phys. Rev. **114**, 1368 (1959), have discussed pair production by high-energy electrons as a possible test of the electron or muon vertex and the photon

processes are shown in Fig. 1. The virtual photon with momentum  $t$  is space-like in diagrams 1(c) and 1(d) but time-like in diagrams 1(a) and 1(b). The detailed calculation of the Bethe-Heitler graphs and complete numerical results which allow for the form factors and recoil of the nucleus, polarized leptons, and exchange terms for identical leptons will be reported elsewhere.<sup>3</sup> For simplicity, we discuss here the characteristic fea-

propagator in the spacelike region. F. Ternovskii, Zh. Eksperim. i Teor. Fiz. **37**, 793 (1959) [English transl.: Soviet Phys.—JETP **10**, 565 (1960)]; M. Chen, Phys. Rev. **127**, 1844 (1962); E. Johnson, *ibid.* **140**, 1005 (1965); and references therein considered various integrated trident cross sections in various situations.

<sup>3</sup> S. J. Brodsky and S. C. C. Ting (to be published).

tures of the triple coincidence cross section

$$d^5\sigma/d\Omega_1 d\Omega_2 d\Omega_3 dE_1 dE_2,$$

assuming that the nucleus acts once as a static potential,<sup>4</sup> the Compton graph can be ignored,<sup>5</sup> and all spins are summed over. For convenience, we consider a muon producing an electron pair,

$$\mu + Z \rightarrow \mu + Z + e^+ + e^-, \quad (1)$$

although most of our results will hold for all four variations.<sup>6</sup>

In this paper we try to determine configurations which will insure that the diagrams 1(a) and 1(b) give the dominant contribution to the cross section and at the same time give a production rate which is large enough so that experiments with present machines may be performed. We thus try to obtain maximum sensitivity to possible modifications of quantum electrodynamics for the time-like momentum region above 100 MeV/c.

We have found it convenient to first select configurations whereby (A), the electron-positron pair is detected symmetrically with respect to the muon scattering plane and (B), the total momentum of the three final leptons is in the incident  $\mu$  direction. Since the nucleus is assumed to be a static potential, the total energy of the three leptons is equal to the energy of the incident particle. Requirement (A) implies that the interference contribution between the space-like diagrams 1(c) and 1(d) and the time-like diagrams 1(a) and 1(b) vanishes since it is antisymmetric under the interchange of the electron and positron momenta,

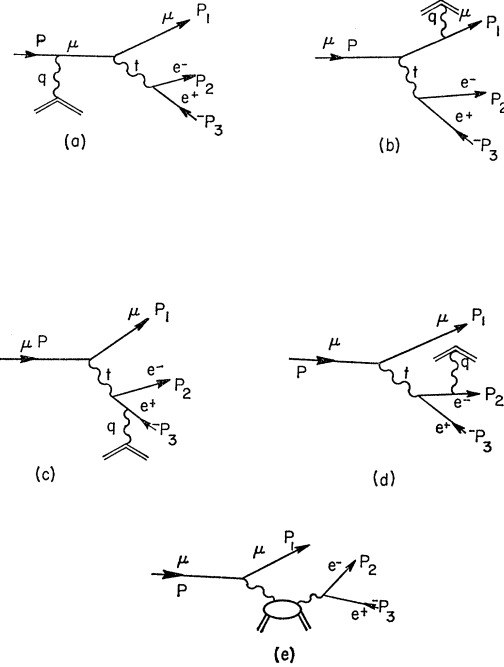


FIG. 1. Lowest order Feynman diagrams for the trident process of Eq. (1). Figures 1(a) to 1(d) give the Bethe-Heitler (Born approximation) contribution. Figure 1(e) represents the general Compton contribution.

whereas the cross section is invariant for mirror symmetry.<sup>7</sup> Requirement (B) insures that the momentum transfer to the nucleus is minimized for fixed lepton energies and polar angles:

$$-q^2 = -(P - P_1 - P_2 - P_3)^2 = q_z^2 \cong (E_1\theta_1^2/2 + E_2\theta_2^2)^2,$$

(assuming small angles and zero lepton mass). With an incident 10-BeV/c  $\mu$  beam and  $\theta_1 \cong \theta_2 \cong 0.1$  rad, we have  $q_z \cong 50$  MeV/c. Thus, even in a high-energy experiment, the nucleus acts as a Coulomb source, requiring only small unambiguous recoil and form factor corrections, and the cross section is nearly proportional to  $Z^2$ . Feasible rates for a muon beam can in fact be obtained from a high- $Z$  target if we choose events with  $|q| \lesssim 80$  MeV/c. As an illustration, we give results for  $Z=10$ , where the Born approximation should still be reliable.<sup>4</sup>

The triple coincidence cross section for the Bethe-

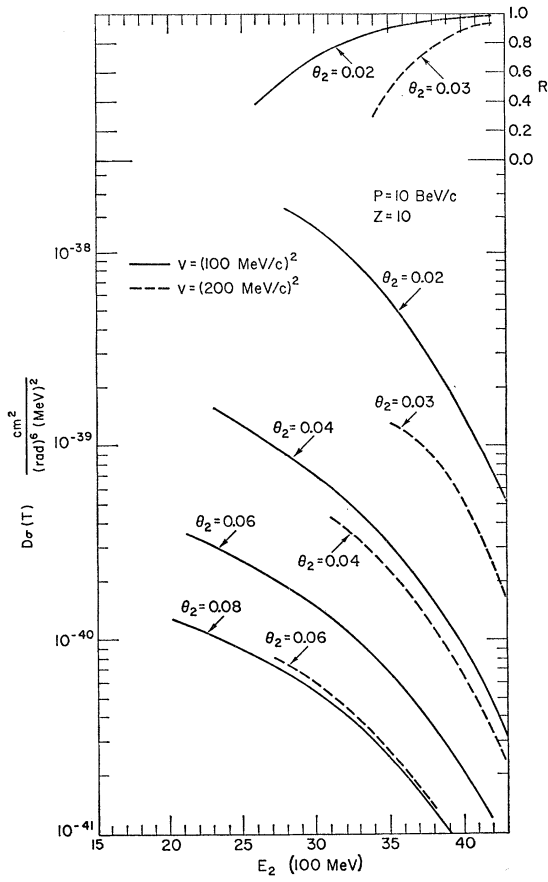
<sup>4</sup> Corrections to Born approximation, due to higher order Coulomb interactions, can be readily estimated from the work of L. C. Maximon and H. A. Bethe, Phys. Rev. **87**, 156 (1952) on photopair production and bremsstrahlung. The corrections are in general of order  $(Z\alpha)^2$  but become negligible if the momentum transfer to the nucleus is small compared to the lepton mass or the lepton momenta transverse to the photon direction. Radiative corrections for the trident process are expected to be of order 10%.

<sup>5</sup> In contrast with the photoproduction of symmetric pairs, the Compton graph, Fig. 1(e), does interfere with the timelike Bethe-Heitler graphs but still the contribution is estimated to be less than 2%. The smallness of this interference term (as well as higher order Born terms and radiative corrections involving three electromagnetic interactions of the lepton current) can be readily checked experimentally when the timelike graphs dominate by using both polarities of the incident beam since the interference term with the timelike graphs is proportional to the charge of the incident beam.

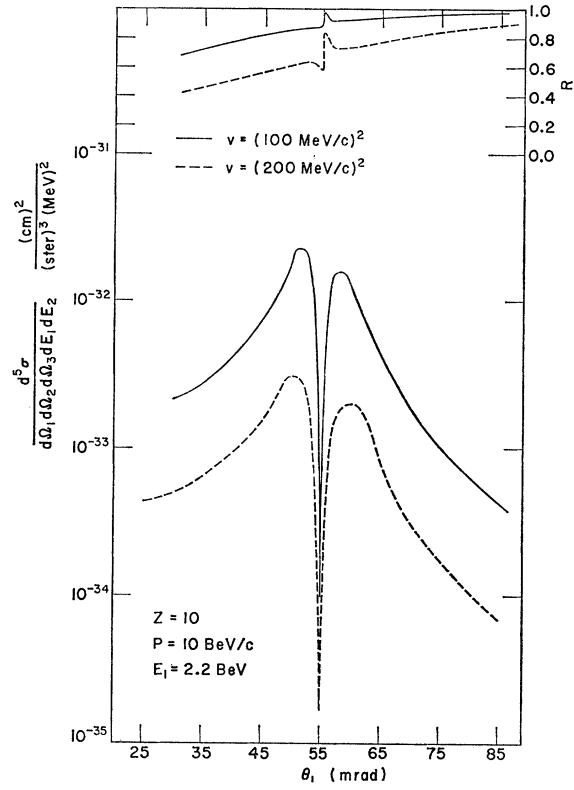
Following A. Krass, Phys. Rev. **138**, B1268 (1965), one can suppose that the size of the Compton term is characterized by a peripheral graph, whereby the virtual photons interact with the nucleus via one pion exchange, and the leptonic pair come from the electromagnetic decay of a vector meson. However, in comparison with the Bethe-Heitler rate, the peripheral contribution is reduced by the factor  $q^2/M_\pi^2 \lesssim 0.01$  (from the pion-nucleon interaction) and by roughly a factor of  $Z$ . Furthermore, whereas the Bethe-Heitler trident cross section increases rapidly for small angles, the contributions from Compton graphs are comparatively angle-independent.

<sup>6</sup> If an electron beam is used, the experimental analysis will be complicated by pairs produced by bremsstrahlung.

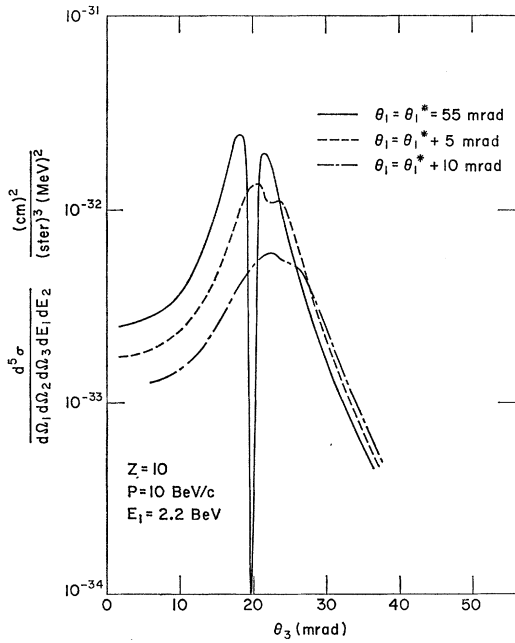
<sup>7</sup> The proof of antisymmetry is similar to the proof of Furry's theorem since the trace required for this interference term also occurs in the matrix-element evaluation of a closed electron loop with three electromagnetic interactions. Since spins are not measured, the symmetry condition (A) implies that the cross section is invariant under the interchange of the electron and positron momenta. The interference term thus gives no net contribution even for finite acceptance, if the events are collected symmetrically. A similar situation is described by J. D. Bjorken, S. D. Drell, and S. C. Frautschi, Phys. Rev. **112**, 1409 (1958) concerning the interference of Compton and Bethe-Heitler graphs for photopair production.



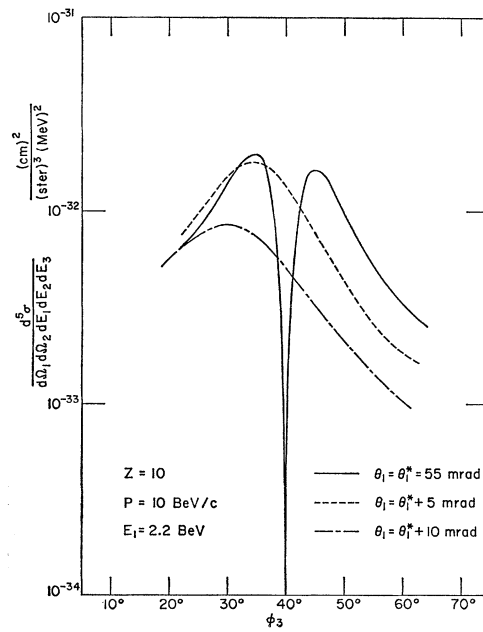
(a)



(b)

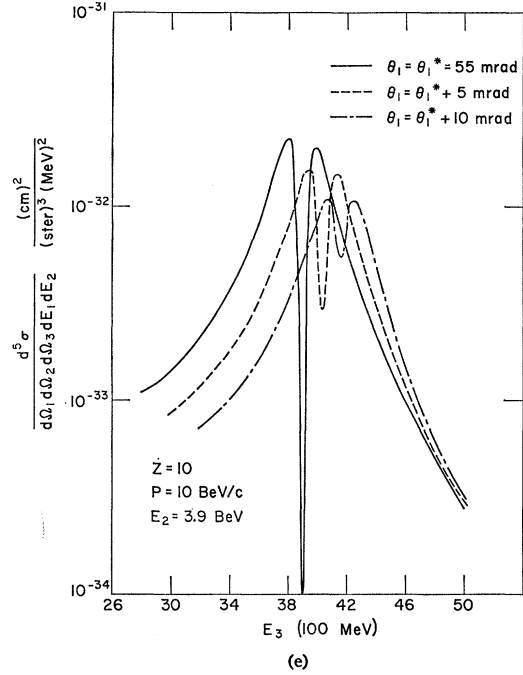


(c)



(d)

FIG. 2. Properties of the cross section of process (1) in the time-like region for incident momentum of 10 BeV/c and nuclear charge,  $Z=10$ . (a): Behavior of the partial cross section  $D_\sigma(T)$  due to time-like graphs 1(a) and 1(b) and the ratio  $R$  of this contribution to the total trident cross section under the restrictive symmetry requirements (A) and (B) of the text. (b): Behavior of the cross section and the ratio  $R$  when requirement (B) is relaxed, i.e.,  $\mathbf{q}$  not restricted to the incident direction ( $\theta_1 \neq \theta_1^*$ ). The curves in 2(a) and (b) are shown for virtual photon time-like momenta squared  $v=(100 \text{ MeV}/c)^2$  and  $v=(200 \text{ MeV}/c)^2$ . (c), (d), (e): Behavior of the cross section for  $v=(100 \text{ MeV}/c)^2$  when requirements (A) and (B) are both relaxed by varying the positron coordinates from the mirror symmetrical arrangement. The three curves plotted in each figure correspond to the three fixed values of  $\theta_1$ . For  $\theta_1 = \theta_1^*$  the minima in these curves correspond to the cross section with exact symmetry conditions (A) and (B). All points shown in Fig. 2 have  $|\mathbf{q}| < 80 \text{ MeV}/c$ .



Heitler diagrams can be written as<sup>8</sup>

$$\frac{d^5\sigma}{dE_1 dE_2 (d\Omega)^3} = \frac{P_1 P_2 P_3 Z^2 \alpha^4}{P} \frac{1}{2\pi^4} \times (m_\mu m_e)^2 \sum_{\text{spin}} |M_s + M_t|^2 \frac{1}{q^4}, \quad (2)$$

where

$$M_t = M_a + M_b = \bar{u}(P_1) J_t^{\mu} u(P) \bar{u}(P_2) \gamma_{\mu} v(P_3), \quad (3)$$

$$M_s = M_c + M_d = \bar{u}(P_1) \gamma_{\mu} u(P) \bar{u}(P_2) J_s^{\mu} v(P_3), \quad (4)$$

and  $\bar{u}(P_1) J_t^{\mu} u(P)$ ,  $\bar{u}(P_2) J_s^{\mu} v(P_3)$  are the time-like and space-like conserved currents:

$$J_t^{\mu} = (-\gamma^{\mu} \mathbf{q} \gamma_0 \omega_3^{-1} + \gamma_0 \mathbf{q} \gamma^{\mu} \omega_4^{-1}) + 2\gamma^{\mu} (E\omega_3^{-1} + E_1 \omega_4^{-1}), \quad (5)$$

$$J_s^{\mu} = (\gamma_0 \mathbf{q} \gamma^{\mu} \omega_1^{-1} + \gamma^{\mu} \mathbf{q} \gamma_0 \omega_2^{-1}) + 2\gamma^{\mu} (E_2 \omega_1^{-1} + E_3 \omega_2^{-1}),$$

with

$$\bar{u}(P_1) J_t^{\mu} u(P) (P_2 + P_3)_{\mu} = 0; \quad \bar{u}(P_2) J_s^{\mu} v(P_3) (P_1 - P)_{\mu} = 0. \quad (6)$$

The  $\omega$ 's are defined by

$$\begin{aligned} \omega_1 &= (P_1 - P)^2 (q^2 + 2P_2 \cdot q), \\ \omega_2 &= -(P_1 - P)^2 (q^2 + 2P_3 \cdot q), \\ \omega_3 &= (P_2 + P_3)^2 (q^2 - 2P \cdot q), \\ \omega_4 &= (P_2 + P_3)^2 (q^2 + 2P_1 \cdot q). \end{aligned} \quad (7)$$

<sup>8</sup> The notation is given in J. D. Bjorken and S. D. Drell, *Relativistic Quantum Fields* (McGraw-Hill Book Company, Inc., New York, 1965).

For many purposes the above expression is the most practical form for the numerical calculation<sup>9</sup> of the cross section since in this form large cancellations of gauge-variant quantities do not occur.

However, if we apply the requirements (A) and (B), the cross section is obtained in a relatively simple analytical form

$$\begin{aligned} D_\sigma(T) + D_\sigma(S) &\equiv \frac{d^5\sigma}{dE_1 dE_2 (d\phi)^3 (d\theta)^3} \\ &= \frac{Z^2 \alpha^4 P_1 P_2 P_3}{2\pi^4 P} (S + T) \frac{\sin\theta_1 \sin^2\theta_2}{q^4}, \end{aligned} \quad (8)$$

where

$$\begin{aligned} S &\equiv (m_e m_\mu)^2 \sum_{\text{spin}} |M_s|^2 \\ &= -4(P_1 - P)^2 (P_{2x}^2 + P_{2y}^2) q_z^2 \omega_1^{-2}, \end{aligned} \quad (9)$$

$$\begin{aligned} T &\equiv (m_e m_\mu)^2 \sum_{\text{spin}} |M_t|^2 \\ &= \frac{1}{2} (P_2 + P_3)^2 [(\alpha^2 + \beta^2) (2P_1 \cdot P) + 4\alpha\beta\delta \\ &\quad - 4m_\mu^2 \beta^2 + 4m_\mu^2 q_z^2 (\omega_3^{-2} + \omega_4^{-2})] + \frac{1}{2} (P_2 - P_3)^2 \\ &\quad \times [(\alpha^2 + \beta^2) (P_1 \cdot P) + 2\alpha\beta\delta + m_\mu^2 (\alpha^2 - \beta^2)], \end{aligned} \quad (10)$$

with

$$\begin{aligned} \alpha &= q_z (\omega_3^{-1} + \omega_4^{-1}), \\ \beta &= -2(E\omega_3^{-1} + E_1 \omega_4^{-1}), \\ \delta &= E_1 P_z - E P_{1z}. \end{aligned} \quad (11)$$

<sup>9</sup> We find that for computer calculations it is more efficient to multiply the Dirac matrices directly instead of using the usual reduction formulas.

If we ignore the lepton mass in the numerators of (9) and (10),<sup>10</sup>

$$S = 8(P_{2x}^2 + P_{2y}^2)(P_1 \cdot P)q_z^2 \omega_1^{-2}, \quad (12)$$

$$T = (P_2 \cdot P_3)(P_1 \cdot P)(\alpha + \beta)^2. \quad (13)$$

The behavior of  $S$  and  $T$  can best be understood by considering the incident energy  $E$ , the pair angle  $\theta_2$ , and the desired momentum-transfer squared of the time-like photon,  $v = (P_2 + P_3)^2$ , to be parameters, and letting the final electron energy, muon energy, or muon angle be an adjustable variable to insure a large time-like-to-space-like ratio  $T/S$  and large cross section. If we consider only small angles and ignore lepton mass, then (12) and (13) give

$$\frac{d^8\sigma}{dE_1 dE_2 (d\phi)^3 (d\theta)^3} = \frac{Z^2 \alpha^4 16(1+S/T) \lambda^{3/2} (2+r)^2}{2\pi^4 E^4 \theta_2^5 \bar{v} (2+\lambda r)^6}, \quad (14)$$

with

$$S = [E_2^2 \lambda r (r+2)]^{-1}, \quad T/S = \lambda^2 / [\bar{v} (2+\lambda r)^2], \quad (15)$$

where the two variables

$$\lambda \equiv \theta_1^2 / \theta_2^2 \quad \text{and} \quad r \equiv E_1 / E_2 \quad (16)$$

are constrained by

$$\bar{v} \equiv v / E^2 \theta_2^2 = (4 - \lambda r^2) / (r+2)^2. \quad (17)$$

It is readily seen from Eqs. (14)–(17) that the optimal condition for large  $T/S$  is given by large  $\theta_1$  [and hence small  $E_1$  to satisfy condition (B)]. In Fig. 2(a) we have shown  $D_\sigma(T)$  [as calculated from Eqs. (8) and (10)] and  $R$ , the fraction of the total trident cross section due to the square of the time-like graphs, as functions of  $E_2$  with  $\theta_2$  and  $v$  as parameters. Although the ratio  $R$  decreases slowly with decreasing  $E_2$ , the partial cross section  $D_\sigma(T)$  increases rapidly.

It must be emphasized that the cross sections presented so far, although remarkably simple, are only valid when the symmetry conditions  $A$  and  $B$  are imposed. The requirement that  $\mathbf{q}$  is in the incident direction in fact minimizes the rate. In Fig. 2(b) it is shown that if the direction of  $\mathbf{q}$  is perturbed by varying  $\theta_1$  by 1 mrad, the cross section increases by a factor of

200. This feature holds quite generally at every point of Fig. 2(a): the maxima obtained by slightly relaxing condition (B) are roughly proportional to the minima.

The same feature of the cross section is seen in Figs. 2(c), (d), and (e) where conditions (A) and (B) are relaxed as the momentum of the positron is changed. As in Fig. 2(b), the ratio  $R$  is found to remain large.

The trident cross section is suppressed for  $\mathbf{q}$  in the incident direction because of a selection rule against the transverse polarization contributions of the virtual photon. If  $\mathbf{q}$  is in the  $z$  direction the matrix element for virtual transverse photons in the forward direction tends to vanish by angular-momentum conservation since the muon helicity is conserved in a series of vector interactions at high energies. The pairs produced by this transverse photon are further suppressed in the forward direction since high-energy vector interactions require the electron and positron to have opposite helicities.<sup>11</sup> The total time-like and longitudinal polarization contributions is small since the photon is relatively close to the mass shell.

We have also shown the variations of the cross section for  $\theta_1$  fixed at 5 and 10 mrad above the symmetry angle  $\theta_1^*$ , thus giving configurations where the cross section is large but slowly varying. The cross section is nominally  $10^{-32} \text{ cm}^2 / (\text{MeV})^2 (\text{sr})^3$  at  $P = 10 \text{ BeV}/c$ ,  $Z = 10$ ,  $v = (100 \text{ MeV}/c)^2$  for ranges  $\Delta\theta_1 \cong \Delta\theta_2 \cong \Delta\theta_3 \cong 20 \text{ mrad}$ ,  $\Delta\phi_2 \cong \Delta\phi_3 \cong 40^\circ$ ,  $\Delta E_1 \cong \Delta E_2 \cong \Delta E_3 \cong 1 \text{ BeV}$  with the ratio  $R$  above 0.8. Therefore favorable rates for experiments sensitive to the time-like region are possible.

In summary, we note that a triple coincidence measurement of reaction (1) in the kinematic region described in this paper enables one to study the quantum electrodynamics of the photon propagator and the vertex function in the time-like region above  $100 \text{ MeV}/c$ . We further note that an important test of  $\mu$ - $e$  universality in the time-like region can also be easily performed by measuring three muons in the final state, taking into account mass differences and statistics.<sup>3</sup>

The authors wish to acknowledge valuable discussions with Dr. M. Kugler, Professor L. M. Lederman, and Professor D. R. Yennie.

<sup>10</sup> This still gives the cross section within 10%.

<sup>11</sup> J. D. Bjorken and S. D. Drell, Ref. 2.